Plastic buckling of short cylinders with axial temperature distribution under transverse shearing loads

H.Nakamura, S.Matsuura & A.Sakurai
Central Research Institute of Electric Power Industry, Chiba, Japan

Abstract

Vertical short cylindrical shells which are subjected to horizontal seismic loads can fail by buckling in shear. Radius-to-thickness ratio and length-to-radius ratio of the main vessel of pool-type LMFBR are estimated about 200 and 0.9 thru 1.1, respectively. However, there is very little information of plastic shear buckling strength of the geometries.

The purpose of this paper is to describe the test results and some considerations on plastic shear buckling of short cylinders. The models have a nominal diameter of 1000mm, nominal length of 500mm and 600mm, and shell thickness of 2.5mm with axial temperature distribution.

1. Introduction

Following up feasibility study (1981 thru 1983) to make certain that the pool-type LMFBR is feasible in Japan located in an earthquake prone zone, Central Research Institute of Electric Power Industry has been proceeding with technical assessment study (1984 thru 1986) in cooperation with Toshiba Corp., Mitsubishi Ltd. and Hitachi Ltd. in Japan, in order to accomplish cost reduction of reactor structure and enhanced structural reliability. One of the themes in the study is to contribute to rational and economical design by clarifying the seismic buckling behaviors of the pool-type LMFBR main vessel, core support cylinder, etc.. For this purpose, buckling tests and numerical analyses were carried out. This paper outlines the buckling test results of short cylinders with temperature distribution under transverse shearing loads.

Concerning the buckling strength of the pool-type LMFBR, experimental buckling data under transverse shearing loads are the most scarce and critical. Pool-type reactors have their main vessel cylinders estimated at radius-to-plate thickness ratio (R/t) of approximately 200, length-to-radius ratio (L/R) of 0.9 thru 1.1 and cylinder root bending stress-to-shear stress ratio (σ_b/τ) of 0.8 thru 1.3 in Japan. A total of 20 cylindrical shell models having R=500 mm, R/t=200 and L/R=1.0 and 1.2, made of type 304 stainless steel, were used for shearing buckling tests. The temperature conditions were shown in Table 1.

These tests were aimed at directly clarifying the buckling stresses of main vessel cylinders against horizontal forces. Especially, in order to clarify the shear buckling strength of real vessels under the working conditions, buckling loads, buckling modes and physical properties of the stainless steel at the room temperature, 200℃, 350℃ and 400℃ were obtained. At the same time, it was also intended to obtain the fundamental data, such as restoring force characteristics after buckled, for a study of dynamic post buckling behaviors under seismic forces.

2. Buckling Test Setup and Models

The buckling test setup is shown in Fig. 1. The screw jack (not hydraulic) has horizontal load capacity of 100 metric tons. Transverse shearing loads were applied via the jack to the upper flange of the specimen fixed on the floor. The (σ_b/τ) ratios of 1.6 and 1.8 were chosen in these tests.

The specimens are shaped as shown in Fig. 2. The test cylinders were finished by welding after rolling the stainless steel plates. At both upper and lower ends, the cylinders were welded to flanges, and 100 mm wide from the welding line was clamped with belts and bolts.

Measuring items were cylinder plate thickness, material physical properties, shape imperfections, loads, displacements, strains and temperatures.

In the tests, special consideration was given to addition of axial tensile stress and of temperatures. Axial tensile stress relates to the tensile stress due to dead load on real structure. A total of 16 locations were controlled to preset temperature normally within error range of±2℃ with heaters installed inside the cylinder.

3. Test Results and Considerations

Table 1 shows the results of measuring the plate thickness at a total of 180 points at intervals of 10° circumferentially on five cross-sections. It was confirmed that the plate thickness nearly as specified was obtained. Shape imperfection was also measured on five cross-sections and it was confirmed that deviation from a truly round circle was within a range of 1.3 mm at the maximum (see Fig. 3). Fig. 4 is a bar graph showing the frequency components of the deviation. As recognized from the figure, the frequency components of the deviation dispersed properly without any predominant frequencies. Temperatures were distributed uniformly or vertically. In the case of vertically distributed temperature, the specimen was assumed to have a uniform temperature in the upper half while linearly decreased in the lower half. Fig. 5 shows an example of the temperature distribution concerning the case of 200℃. Dupricate tests were made for confirming the repeatability of the buckling loads for this problem. Some remarkable results are summerized as follows:

(i) The maximum loads are governed by the shear buckling mode as shown in Figs. 6 and 7, and circumferential wave numbers are 10 thru 12 (Fig. 8). As the post-buckling deformation increased, secondary mode appeared on the root of compression side due to bending moment

(ii) Material test results are shown in Table 4. The buckling stress reduction at higher temperature is much more highly correlative with decrease in 0.2% proof stress than that with decrease in Young's modulus. Buckling under transverse shearing loads took

place at approximately 80% thru 90% of the 0.2% proof stress.

(iii) Buckling wrinkles tend to appear on those higher temperature zone which is weak materially. Buckling loads, however, are not so sensitive to shape imperfection but significantly affected by changes in material properties.

(iv) An example of hysteretic post-buckling characteristics under cyclic loads is shown in Fig. 9. The post-buckling load decreased more slowly than that in buckling under axial compression. The higher the temperature, the more conspicuous that tendency. The load direction was reversed at 3, 4 and 5 times as large as horizontal buckling displacement. When load worked in the opposite direction for the first time, the maximum load was found to be nearly equal to a first buckling load.

(v) An upward tensile force equivalent to the dead weight did not affect the buckling load itself. Nevertheless, it contributed to the suppression of post-buckling load decrease and to the stabilization of post-buckling behaviors.

Considering from the standpoint of design, the ϕ-Method was examined for its validity.

$$\frac{1}{\tau_{ET}^{\,2}} + \frac{1}{\tau_{y}^{\,2}} = \frac{1}{\tau_{p}^{\,2}} \qquad (1)$$

where, τ_{ET} : $0.74E(R/L)^{0.5}(t/R)^{1.25}$ elastic shear buckling stress

τ_y : $\sigma_{0.2}/\sqrt{3}$,shear yield stress ($\sigma_{0.2}$: 0.2% proof stress)

τ_p : plastic shear buckling stress

At room temperature, 200℃ and 350℃, it could be confirmed that the method allowed to estimate roughly (within 7%) the buckling loads. However, some problems have remained still unsolved, including how the Method be applied in the case of distributed temperature.

4. Comparison of Experiment and Numerical Analysis

MARC (No.4 Element :4 node doubly curved shell element) was used to carry out the analysis. Taking advantage of symmetry with respect to the plane which contains loading and cylinder axes, 180° models were employed, being divided into 10 elements heightwise and 20 elements circumferentially. The cylinder was fixed at the lower end, and was stiffened by the rigid ring at the upper end. Forced displacements were applied to the ring horizontally. The forced displacement increments were 0.1 mm while load-displacement relation remained fairly linear. And it was gradually decreased to 0.02 mm in the vicinity of the buckling load. Stress-strain relations were given on a multi-linear approximation basis according to the results of material tests at each temperature.

The shape imperfections given were up to 14 circumferential wave number, based on the observed buckling modes. And the maximum shape imperfections were assumed as 1.25 mm (half the plate thickness), based on the imperfection measurement results. A shape imperfections were given as a sine curve in the vertical direction, assuming no imperfections at both upper and lower ends.

Fig. 10 shows examples of the numerical analysis results. For buckling load, the numerical values were a little larger than the experimental values (approx. 10% thru 20%), tending to show a steeper gradient of the load-displacement curve. For the post-buckling load,

the numerical values are also smaller. The shape imperfections have effects of lowering the buckling loads. It is not a factor, however, so controlling as to drastically reduce the buckling loads.

At present, it is difficult to use the numerical values to estimate buckling loads of cylindrical shells under transverse shearing loads. Nevertheless, it seems applicable to the sensitivity analyses of the factors which influence the buckling.

5. Conclusion

Concerning the shear buckling on pool-type LMFBR cylindrical shells, a study has been made as reported above. Parameters, such as R/t and L/R ratios, temperature conditions, etc., however, were limited. The authors believe that sufficient test data should be accumulated from time to time in parallel with design study on demonstration reactors in Japan. The following problems are left to be clarified:

(i) Buckling behavior under the coupling loads, including a thermal one.

(ii) Buckling behaviors under the dynamic loads, and the quantitative evaluation of the effects of the seismic forces.

(iii) Quantitative evaluations of various imperfections.

In addition, it is urgently necessary to develop the specially designed buckling analysis codes.

References

1) Central Research Institute of Electric Power Industry : Feasibility Study on Large Pool-type LMFBR - The Final Report -, Report No.A01, July,1984 (in Japanese)
2) T. Murakami, et al.: Buckling Strength of Elliptical Heads with Core Support Structure under Vertical and Horizontal Loads, 9th International Conf. on SMiRT, E4/4
3) Y. Kawamoto, et al.: Plastic Buckling of Short Cylinders under Transverse Shearing Loads, 9th International Conf. on SMiRT, E4/9, 1987
4) K. Kokubo, et al.: Buckling Behaviors of Short Cylindrical Shells under Dynamic Loads, 9th International Conf. on SMiRT, E4/2, 1987
5) Galletly, G. D. and BLachut, L.: Plastic Buckling of Short Vertical Cylindrical Shells Subjected to Horizontal Edge Shear Loads, Transactions of ASME, Journal of Pressure Vessel Technology, Vol.107, May 1985
6) Yamaki, N. : Elastic Stability of Circular Cylindrical Shells, North-Holland, 1984

Table 1 Buckling test cases

Number of Tests	Temperature Conditions
6	uniform room temperature (about 20 ℃)
2	uniform 200 ℃
3	uniform 200 ℃ (upper half), linearly decreased from 200 ℃ to about 60 ℃ (lower half)
2	uniform 350 ℃
5	uniform 350 ℃ (upper half), linearly decreased from 350 ℃ to about 70 ℃ (lower half)
2	uniform 400 C (upper half), linearly decreased from 400 ℃ to about 75 ℃ (lower half)

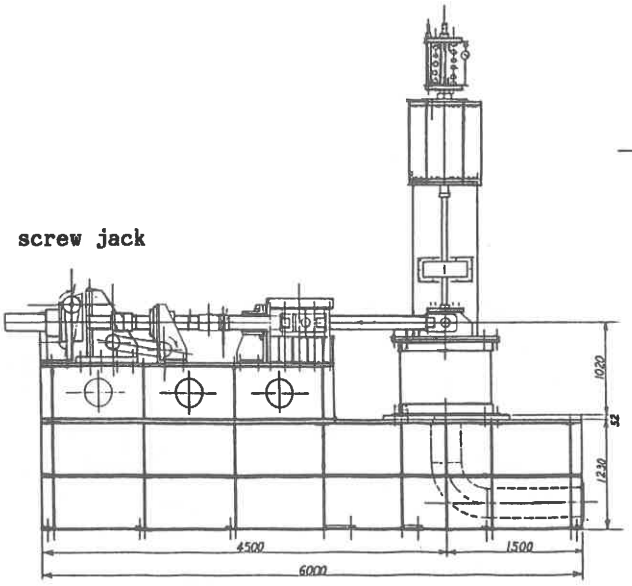

Fig. 1 Buckling test setup

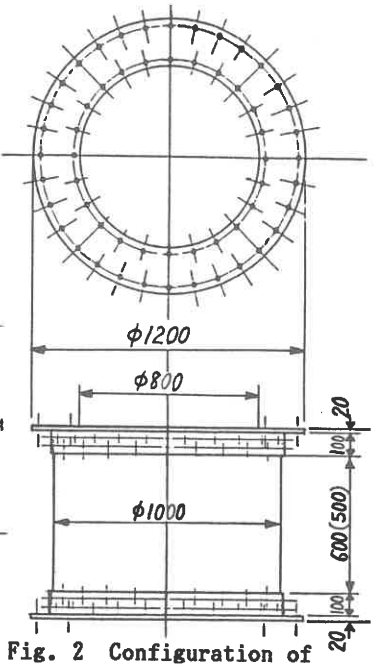

Fig. 2 Configuration of cylinder models

Table 2 Buckling test results

Test No.	Temp.	Axial Force	Buckling Load	Disp.
1	Room	15(Ton)	45.8(Ton)	1.44(mm)
2		15	46.1	1.56
3		0	47.4	1.57
4		0	45.3	1.44
5	200℃ Uniform	15	34.8	1.56
6		15	33.9	1.57
7	200℃ Distributed	15	36.1	1.39
8		15	36.6	1.40
9	350℃ Uniform	15	31.3	1.77
10		15	32.0	1.69
11	350℃ Distributed	15	34.0	1.50
12		15	34.0	1.58
13		0	33.5	1.33
14		0	32.9	1.35
15	400℃ Distributed	15	31.7	1.54
16		15	31.5	1.57
17	Room	15	42.7	1.67
18		15	43.8	1.82
19	200℃ Distributed	15	35.6	1.46
20	350℃ Distributed	15	30.6	1.48

Table 3 Thickness of cylinders

Test No.	Min.	Max.	Average
1	2.46	2.53	2.49
2	2.46	2.52	2.48
3	2.46	2.56	2.50
4	2.44	2.54	2.50
5	2.45	2.53	2.48
6	2.47	2.51	2.49
7	2.46	2.59	2.50
8	2.46	2.54	2.50
9	2.43	2.52	2.48
10	2.46	2.54	2.49
11	2.47	2.54	2.50
12	2.46	2.53	2.49
13	2.47	2.54	2.50
14	2.47	2.53	2.50
15	2.45	2.56	2.48
16	2.45	2.53	2.49
17	2.46	2.53	2.49
18	2.47	2.54	2.50
19	2.46	2.53	2.50
20	2.47	2.54	2.49

(Unit : mm)
(No.1~16: H=500 ; No.17~20: H=600)

Table 4 Physical properties of type 304 stainless steel

Temperature	0.2% Proof Stress (kg/mm²)	Tensile Strength (kg/mm²)	Elongation (%)	Young's Modulus (kg/mm²)	Poisson's Ratio
Room	25.4	66.0	64.0	1.97×10^4	0.27
100℃	21.8	51.9	51.0	1.93×10^4	0.27
200℃	18.4	45.7	40.5	1.88×10^4	0.28
350℃	14.6	42.4	34.8	1.77×10^4	—
400℃	13.8	42.7	34.7	1.72×10^4	—

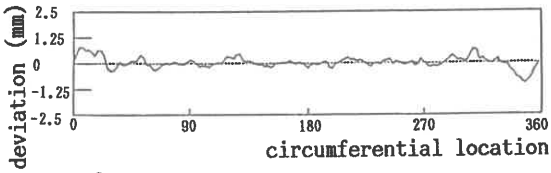

Fig. 3 Deviation from truly round circle

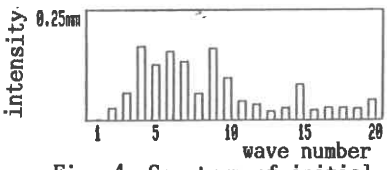

Fig. 4 Spectrum of initial imperfection

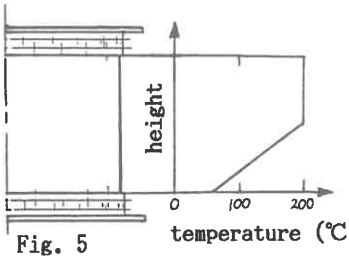

Fig. 5 Axial temperature distribution (200 ℃ distributed case)

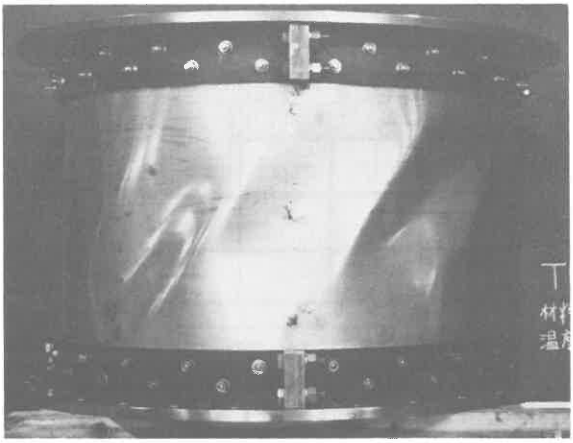

Fig. 6 A buckled cylinder model

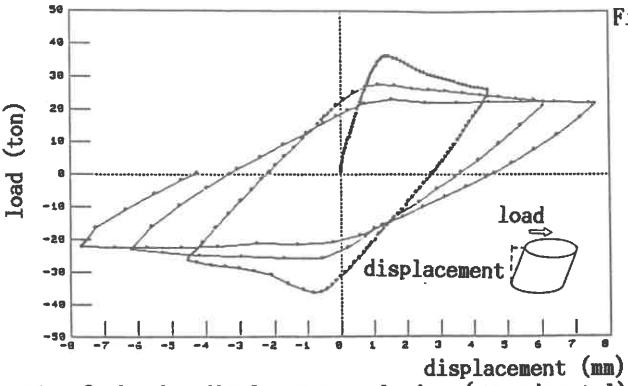

Fig. 9 Load - displacement relation (experimental)

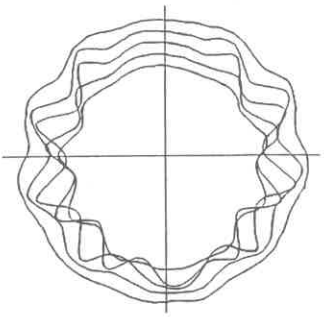

Fig.7 Measured buckling mode shape

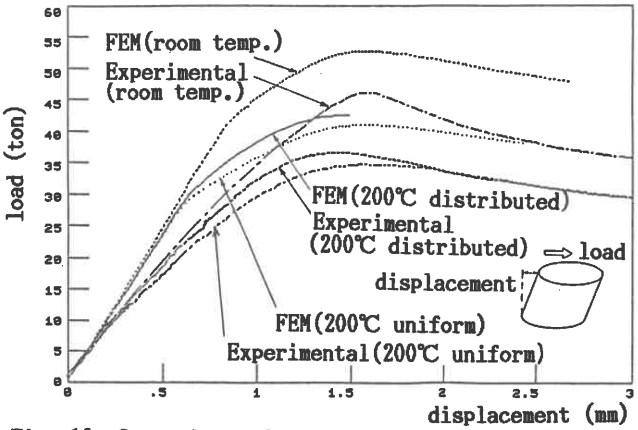

Fig. 10 Comparison of load - displacement relations

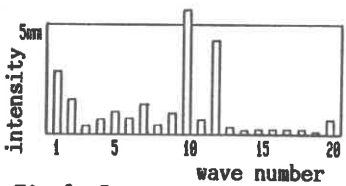

Fig.8 Spectrum of buckling deformation